
6th International Conference on
Case Histories in Geotechnical Engineering, Arlington, VA, August 11-16, 2008

BACK ANALYSIS OF A DEEP EXCAVATION IN SOFT LACUSTRINE CLAYS

Patrick Becker
University of Kassel
Kassel, Germany

Berhane Gebreselassie
University of Kassel
Kassel, Germany

Hans-Georg Kempfert
University of Kassel
Kassel, Germany

ABSTRACT

Up to 9.9 m deep excavation was executed in 2002 for the LAGO Shopping Center in Constance city near the lake Bodensee (Constance lake) located north of the German alps. The excavation was 100 m long and 50 to 100 m wide and carried out in two parts. Part I of the excavation includes two basement floors and part II one basement floor. The underground condition in city Constance and the surroundings is known of a deep and soft deposit of lacustrine clay. To reduce deformations due to excavtaion, the part I was again partitioned in three longitudinal strips by means of intermediate sheet pile walls following the orientation of the pile grid system. The sheet pile walls were supported at the top about -4 m below the ground surface by steel struts and at the bottom of excavation by concrete slabs. Since the bottom support was intended to contribute to safety against basal and overall failure at the same time, it was connected to the piles and supposed to overcome tensile stresses.
The paper shows the effects of the special construction stages followed at the site on the deformation behaviour of the excavation based on numerical analysis using the Finite Element Method (FEM). Furthermore, the time dependant pore pressure development corresponding to the special construction stages is presented. Finally, the numerical results are compared with the field measurement data.

INTRODUCTION

The LAGO Shopping center with two underground basements was built in 2002 in the city of Constance in built in area. The area of the lake Constance, locally known as Bodensee, is known of underground with thick layer of post glacial soft lacustrine deposit. Its thickness is believed to exceed 25 m. Excavation on such thick soft soils in urban areas is associated with large deformations. To avoid excessive deformations, a special construction measure had been taken and the excavation work had been successfully completed (see also *Krieg et al. 2004a,b*). Similar projects in the city Constance and surroundings had been reported by *Goldscheider/Gudehus (1988), Katzenbach et al. (1992), Kempfert/ Gebreselassie (1999), Gebreselassie (2003), Gebreselassie/ Kempfert (2004)* and *Kempfert/Gebreselassie (2006).*

The aim of this paper is to perform a back analysis of the special excavation procedure of the project. In particular, the effect of the special construction measure used on the deformation behaviour and excess pore pressure development will be presented.

GENERAL DESCRIPTION OF THE EXCAVATION SITE

Underground conditions

The ground consists of 5 layers (Fig. 1). The upper most layer is 3.0 to 4.5 m thick fill material (layer I), of which 2 to 3 m was already cut of within the premise of the construction site long time prior to the start of the project. Beneath the fill is a (2.5 to 4.5 m) thick layer (layer II) which consists silty fine to medium sand alternatively and it is underlain by soft lacustrine deposit (upper lacustrine clay, layer III) starting from a depth about -5.5 to -9 m below the ground surface. The lacustrine soil changes its consistency from soft to stiff starting from approximately at a depth of -20 m in the north and -35 m in the south below the ground surface and it strongly consists sand and gravel particles (lower lacustrine clay, layer IV). From a depth of -28 to -32 m in the north and -50 m in the south downwards, the underground is dominated by a ground moraine (layer V).

The upper groundwater level was located at about -3 m below the ground surface during the exploration. A second confined groundwater was also encountered in the ground moraine whose water head reaches up to -1 m below the ground surface.

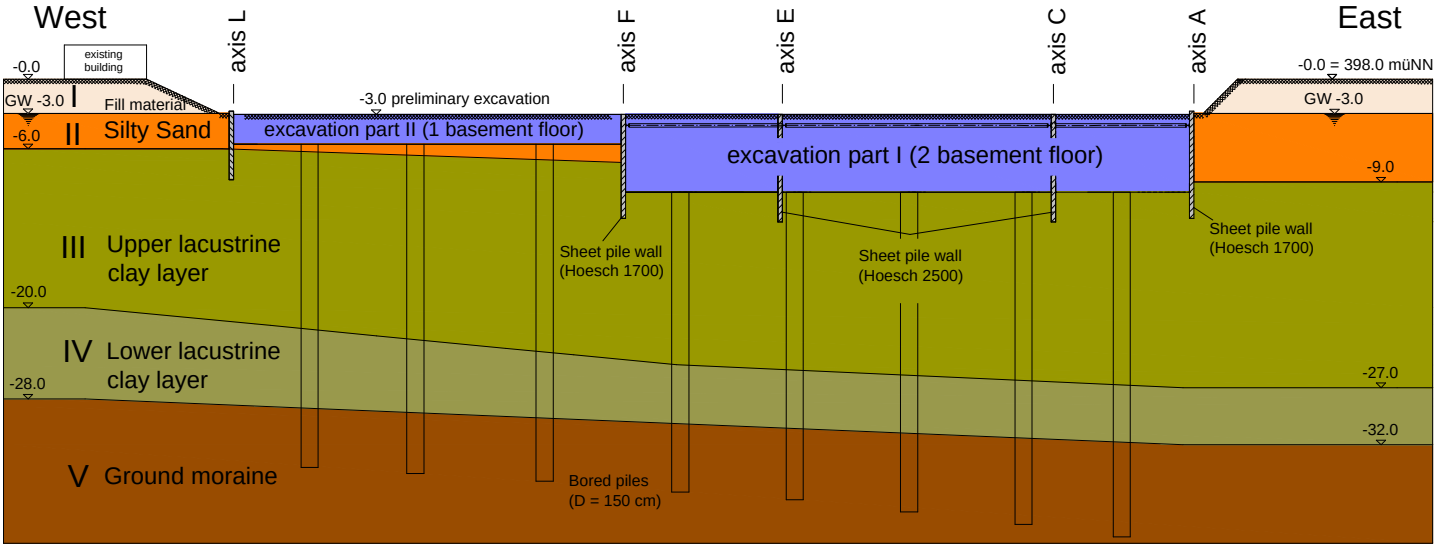

Fig. 1. Section trough the excavation site from west to east and soil profile

The results of a number of field and laboratory soil tests are summarized in Fig. 2 and Fig. 3. The natural water content varies between 35 and 15% and shows a general decreasing trend with depth. The liquid limit in the upper part varies around 40 % which can be classified as lean clay (CL) according to DIN 18196. Starting from a depth of approximately -14 m, the lacustrine soil becomes CL-ML with falling liquid limit value due increasing amount of silt and fine sand.

On the basis of the consistency index I_C (Fig. 3) the intersection from the upper lacustrine clay layer and the lower lacustrine clay layer is obvious at a depth of -20 to -28m. The consistency changes from soft with I_C = 0.1 to 0.4 to stiff with I_C > 0.5.

There were very limited and highly strewing values of the undrained shear strength from the field vane tests available during the preliminary design phase. Therefore, supplementary field vane tests had been conducted during the construction phase and the low undrained strength of the underground had been once again verified.

The normalized undrained shear strength λ_{cu} of normally consolidated clay can be assumed to be constant with the depth, provided that the groundwater is located at relatively shallow depth.

$$l_{cu} = \frac{c_u}{s'_{vc}} = constant \qquad (1)$$

$$c_u = t_f \cdot m \qquad (2)$$

where c_u = the undrained shear strength, σ'_{vc} = effective vertical overburden pressure, τ_f = undrained vane shear strength, and μ = vane correction factor.

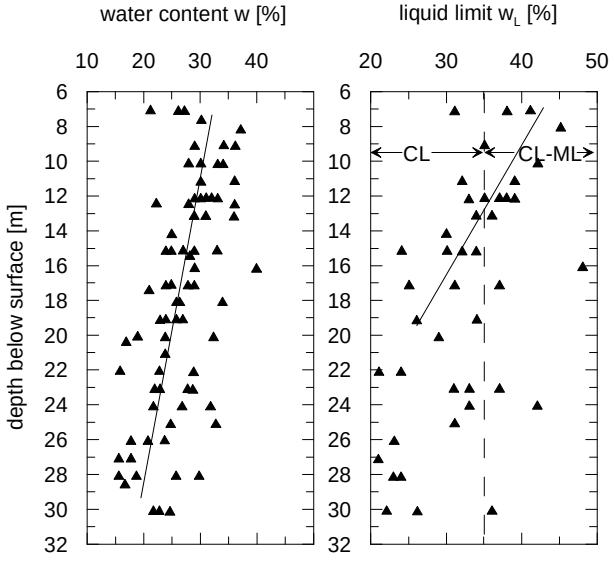

Fig. 2. Profile of water content and liquid limit

The value of λ_{cu} from the field vane shear strength (Fig. 3) and with due consideration of the vane correction factor is found to be 0.13 for the soil up to a depth of -17 m below the ground surface and thereafter 0.18. Comparing these values with empirical relations in the literature (Table 1) for lacustrine soft clay in Constance, there is a large discrepancy. The values of the normalized undrained shear strength by *Scherzinger (1991)* had been derived from triaxial tests on undisturbed samples of lacustrine soft clay in Constance. Whereas *Heil et al. (1997)* determined the values of l_{cu} using both triaxial and field vane

shear tests on similar lacustrine soft clay in the city of Kreuzlingen in Switzerland which is also located in the Alps region. The ratio of the normalized undrained shear strength from vane shear and triaxial tests is calculated to be $l_{cu,vane}/l_{cu,triax}$ = 0.7 according to *Heil et al. (1997)*. Similar value can also be obtained, if one takes the value of l_{cu} = 0.26 from *Scherzinger (1991)* and the vane test results l_{cu} = 0.18 from this project for a depth below -17.0 m. The anisotropy of the normaly consolidated soft lacustrine clay, the stress history and the different direction of load application are probably the reasons for the lower undrained shear strength from field vane tests.

Table 1. Normalised undrained shear strength

Equation	Reference	Region of applicability
$l_{cu} \simeq 0.26$	*Scherzinger (1991)*	lacustrine soft clays (Constance)
$l_{cu} \simeq 0.30$	*Heil et al. (1997)*	lacustrine soft clays (Kreuzlingen, from triaxial tests)
$l_{cu} \simeq 0.20$	*Heil et al. (1997)*	lacustrine soft clays (Kreuzlingen, from vane tests)
$l_{cu} \simeq 0.30$	*Burland (1990)*	natural sensitive clays (remoulded soil)

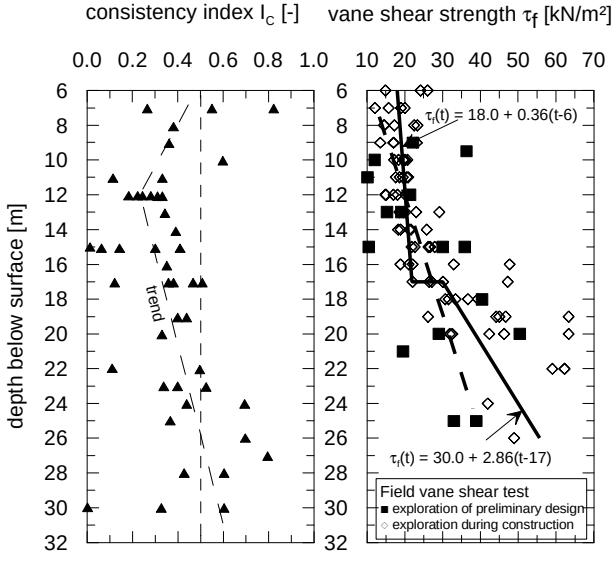

Fig. 3. Consistency index and vane shear strength

Support System

The trapezoidal shaped layout of the excavation (Fig. 4) consists of a rectangular portion (Part I) with an excavation depth of 9.1 to 9.9 m that accommodates two basement floors and a triangular portion (Part II) with a depth of 5.8 to 8.0 m. The two excavation parts were executed successively. The construction plan included the installation of the sheet pile walls first and placement of approximately 130 bored piles with a diameter D = 1.50 m that extend deep into the moraine layer starting from the existing preliminary excavation level at a depth of about -3 m below the ground surface.

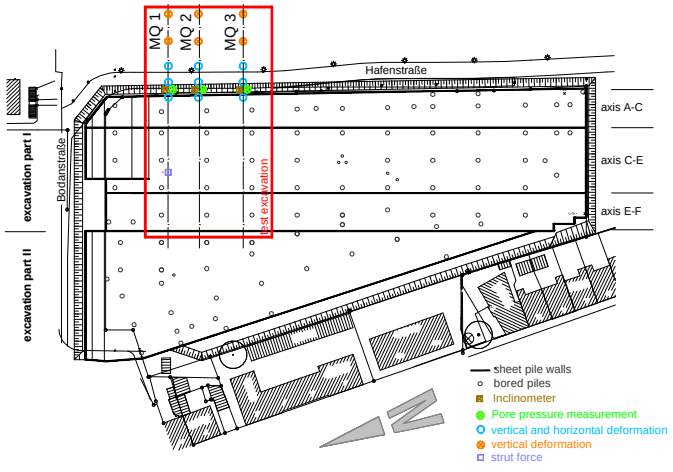

Fig. 4. The site plan and location of the excavation parts

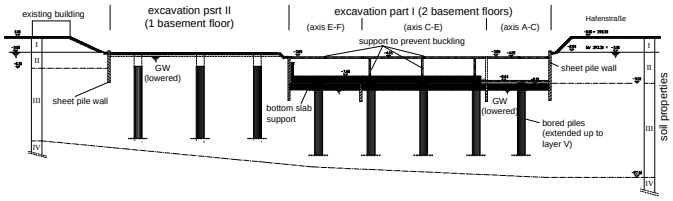

Fig. 5. Section at MQ 1 from west to east, with excavation part I in progress

To avoid excessive deformations in the soft lacustrine layers, the excavation part I was again partitioned in three longitudinal strips by means of intermediate sheet pile walls following the orientation of the pile grid system. The sheet pile walls were supported at the top about -4 m below the ground surface by steel struts and at the bottom of excavation by lean concrete slab and temporary steel struts. Since the bottom support was intended to contribute to safety against basal and overall failure at the same time, it was connected to the piles and it was supposed to overcome tensile stresses, which is reported in *Krieg et al. (2004a)*.

Construction stages

In frame work of the cleaning up operation of the old building rest at the site three years before the beginning of the project, the first pre-excavation had already been executed to a depth of -3.0 m. The installation of the sheet pile walls was followed from this level (Fig. 5). In the excavation part I, an additional pre-excavation was made to a depth of -4.3 m for the placement of the struts and the bored concrete piles.

The excavation of part I was proceeded successively in blocks as shown in Fig. 6. The steps followed are indicated by numbers in the layout. Starting from a slope in the north, the excavation was executed first in the middle strip (Part I, Axes C-E) in slices and immediately followed cutting of the exposed part of the piles and placement of the 0.8 m bottom lean concrete slab on a daily construction capacity basis (Fig. 7). The construction work continued in the outer strip adjacent to the excavation part II and then to the outer strip near the hafen street. Figures 8 and 9 show an overview of the execution of the excavation in strips and blocks according to Fig. 6 at different construction stages.

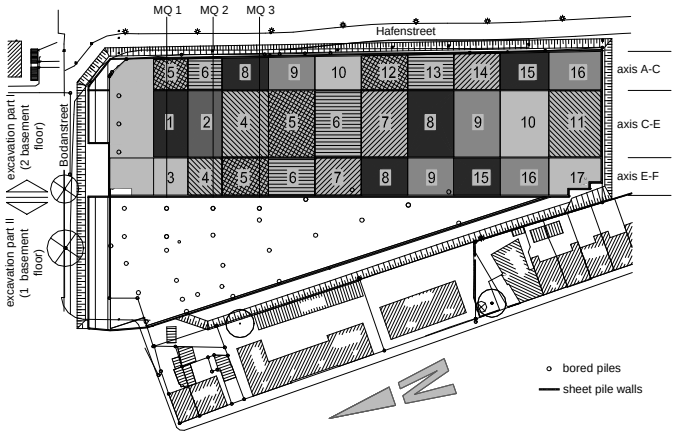

Fig. 6. Layout showing succession of the excavation

The sheet pile walls in the middle strip (24 m wide) of the excavation part I (Axes C-E) were supported using a tied back anchor fixed to the outer sheet piles; hence they formed together a kind of cofferdam effect. With the progress of the excavation, an additional strut was inserted at about a depth of -7.3 m (about 2.5 m above the excavation bottom), which was removed immediately after the placement of the lean concrete bottom slab, see also Fig. 11.

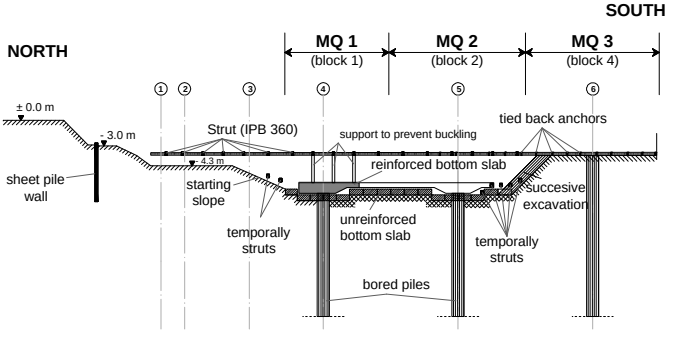

Fig. 7. Section trough the excavation from north to south with construction phases for Axes C-E

In further execution of the excavation, a precast reinforced concrete bottom slab was used instead of cast in-situ lean concrete and hence the time of the construction process had been optimized by avoiding the time required for hardening of the cast in-situ concrete. The precast concrete slab was wedged against the sheet pile walls in order to provide an immediate support to the walls. Immediately after a block (see Fig. 6) had been fully excavated and the lean concrete had been set, a 0.5 to 0.7 m thick reinforced concrete mat was placed.

Fig. 8. Execution of the middle strip till block 2 (Axes C-E)

Fig. 9. Execution of the outer strip adjacent to part II till block 3 (axis E-F)

During the excavation in the neighbouring strips (Axes E-F) with width B = 14 m, the tied back anchors of the walls in the middle strips (Axes C-E) were replaced by steel struts at a depth of –4.0 m with a spacing a = 3 m. To avoid buckling of the struts additional vertical support was provided at the middle of the span using a vertical steel profile which was fixed on

the top of the already completed reinforced concrete. As the excavation proceeded in slices between the Axes E and F, steel struts were inserted at a depth of –4.0 m with a spacing a = 3 m. Thus, the strut reaction forces could be transferred to the opposite sheet pile wall in the Axis C.

Fig. 10. Execution of the strip on Hafen street side till block 6 (axis E-F)

Fig. 11. Details of construction work (axis C-E)

In the outer strip (12 m wide) on the side of the Hafen street (Axes A-C), the struts were already built at head of the wall without any pre-excavation, but with very small trenches. The trenches together with the strut were refilled in order to maintain the work plane for the construction equipments and vehicles (Fig. 10). The excavation then followed stepwise in slices between the struts at the wall head. The wall head was thus supported during the entire stepwise excavation. Immediately after the installation of the struts at the wall head in this strip (Axes A-C), there was a force coherent connection between the walls in the Axes A to E. Thus, there was a transfer of the strut reaction forces due to the excavation to the outer strip (Axes A-C) to the outer wall at Axis E.

Fig. 12. Some details of construction works with slicewise excavation and placement of bottom slab

Figure 11 shows the execution of the partial excavation in the Axes C-E (middle strip) through measurement section MQ1. Further excavation details can also been seen in Fig. 12.

Instrumentation

Since exact prediction of the expected deformations was not possible because of the difficult underground conditions and the associated spatial and temporal soil-structure-interaction, intensive monitoring method was applied. This includes deformation observation using a vertical inclinometer, pore pressure measurements using pressure transducers as well as settlement and position change measurements using geodetic instruments. The observation points were distributed throughout the excavation and arranged in the area of the neighboring Buildings.

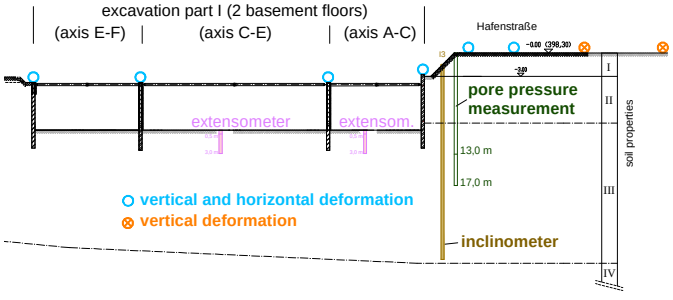

Fig. 13. Instrumentation through MQ 3 at the test excavation pit

In order to prove the carrying capacity of the sheet pile walls and the stepwise excavation, a test excavation pit was made in the excavation part I (Fig. 4). At the test pit the measuring program was supplemented with extensometer and load transducers and the raster of the measuring points was refined (Fig.13).

The monitoring results are presented together with the result of the finite element analysis in the following.

BACK ANALYSIS

The back analysis was carried out using the two-dimensional FE-program PLAXIS 8.2 professional version. This program was specifically developed for geotechnical purposes and it provides material models from simple elastic to advanced elasto-plastic cap models. The hardening soil model (HSM) was used to simulate the behaviour of the soils in all the layers. HSM is based on isotropic hardening and it has the following basic characteristics: stress dependant stiffness according to the power law, plastic straining both due to primary deviatoric loading (shear hardening) and primary compression (compression hardening, cap yield), elastic un/reloading, dilatancy effect and failure according to the Mohr-Coulomb. The contact behaviour was simulated using the Mohr-Coulomb model (MCM) (a simple elastic-perfect plastic model). Detail description of the HSM and the MCM can be found in PLAXIS handbook by *Brinkgreve (2002)* and *Schanz, et al. (1999)*. The structural elements were assumed to behave elastically. A plain strain analysis was adopted using 15 node triangular elements.

Model Geometry and material parameters

Due to the arrangement of the excavation into two parts with different excavation depths and the spatial effect of the stepwise execution in slices in part of the excavation area, the FE-model was built for the entire cross section without taking the advantage of symmetry. The governing cross-section for model geometry is through the monitoring section MQ 3 (Axis 6). However, because of the similarity of the excavation procedure, the model can also represent the cross-section through MQ 1 and MQ 2 of the test excavation, provide that the different construction period is considered.

The excavation part I had a width B = 50 m and a height H = 9.9 m. The extent of the FE-Model was selected to be 3xB = 150.0 m wide on the west side, 2xB = 100.0 m wide on the east side and 5xH = 50.0 m high according to the recommendation of the “Numeric in Geotechnics” of the German Society of Geotechnical Engineers (*Meißner 2002)*.

The material parameters required for the soil models for different layers are given Table 2. The parameters are obtained from the geotechnical investigation report of this project as well as old and actual projects in immediate neighbourhood (*Kempfert + Partner Geotechnik 2006/2007; BBI 2000; Krieg et al. 2004; Gebreselassie 2003; Kempfert/Gebreselassie 2006*).

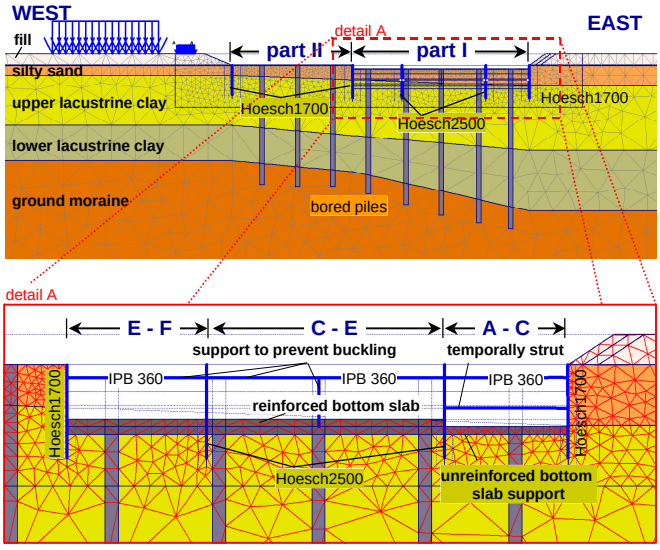

Fig. 12. FE-Model (only an important part of the model is displayed)

Table 2. Soil parameters for the HSM

a) Unit weight and permeability

Soil layer	γ_{sat} [kN/m³]	γ_{unsat} [kN/m³]	$k_x = k_y$ [m/d]
Fill material	21.0	21.0	8.64E-2
Silty sand	20.0	19.0	1.73E-0
Upper lacustrine clay	19.0	19.0	8.64E-4
Lower lacustrine clay	22.0	22.0	8.60E-4
Ground moraine	20.0	20.0	8.60E-4

b) Stiffness parameters

Soil layer	E_{50}^{ref} [MN/m²]	E_{oed}^{ref} [MN/m²]	E_{ur}^{ref} [MN/m²]	p^{ref} [MN/m²]	ν_{ur} [-]	m [-]
Fill material	6.0	6.0	30.0	0.1	0.20	0.70
Silty sand	8.0	8.0	40.0	0.1	0.20	0.50
Upper lacustrine clay	5.0	5.0	25.0	0.1	0.20	0.73
Lower lacustrine clay	8.0	8.0	40.0	0.1	0.20	0.50
Ground moraine	40.	40.0	200.0	0.1	0.20	0.80

c) Shear strength parameters

Soil layer	c´ [kN/m²]	φ´ [°]	ψ´ [°]	R_f [-]
Fill material	0.01	30.0	0.0	0.90
Silty sand	0.01	27.5	0.0	0.90
Upper lacustrine clay	0.01	22.5	0.0	0.90
Lower lacustrine clay	0.01	25.0	0.0	0.90
Ground moraine	0.01	30.0	0.0	0.90

The sheet pile walls, the struts and the temporal tied back anchors in part of the excavation Axes C-E are simulated using a beam element and node ton node anchors respectively.The lean concrete slab, the reinforced concrete slab and the bored concrete piles are idealised with linear elastic continuum elements. The material parameters for the structural elements are given in Table 3 and 4. Since beam elements are wall elements per meter run in out of plane direction, the simulation of the bored concrete piles with beam elements together with impermeable interface elements can lead to a slack of water flow. On the other hand beam elements with permeable interface elements may act as vertical drainage. Both cases can falsify the consolidation calculations substantially. Thus, the bored piles are idealised with linear elastic continuum elements and the permeability values as well as the drainage conditions are taken the same as the corresponding layer. The density and stiffness of the pile for each layer was calculated using an equivalent diameter D_{eq} = 1.32 m according to Eq. (3) and taking into account the pile raster (16.5 x 10.0 m).

$$D_{eq} = \sqrt{D^2 . \frac{p}{4}} \qquad (3)$$

A separate material set was defined for the interface elements according to *Gebreselassie (2003)* und *Kempfert/Gebreselassie (2006)*. Thereby, the shearing strength of the corresponding layer had been reduced depending on the wall friction where as the stiffness had been taken without reduction.

Table 3. Material properties of the structural elements.

Structural element	EA [kN/m]	EI [kNm²/m]	w [kN/m/m]	ν [-]
Sheet pile wall:				
Hoesch 2500	4.053E6	91140.0	1.5	0.30
Hoesch 1700	3.108E6	63210.0	1.2	0.30
Strut: IPB 360	1.267E6	30233.0	0.5	0.30
Tied back anchors (temp.)				
GEWI ϕ = 3.2 cm	1.689E5	$L_{spacing}$ = 3.0 m		

Table 4. Material parameters for linear elastic model

Continuum element	$\gamma_{sat} = \gamma_{unsat}$ [kN/m³]	$k_x = k_y$ [m/d]	ν [-]	E_{ref} [MN/m²]
Lean concrete bottom slab[1)] d = 0.80 m	23.0	0.0	0.20	3.2E4
reinforced bottom slab [1)] d = 0.70 m	25.0	0.0	0.20	3.2E4
Bored piles[2)]	25.0[3)]	[4)]	0.20	3.2E4[3)]

[1)] Non-porous; [2)] drained or undrained depending on the surrounding soil layer; [3)] modified, according to surrounding soil layer and pile raster; [4)] the same as the surrounding soil layer

In the FE computation, the lacustrine clay layers are assumed to behave undrained whereas the ground moraine, the fill and silty sand layers are assumed to behave drained.

Calculation phases

The numerical computations are carried out representative for the cross-section through monitoring section MQ 3. Table 5 shows the construction stages followed in the computation.

Table 5. Calculation phases

Phase				
01	P	generate the initial stresses with gravity loading		
02	P	activate the surcharge loads		
03	P	1st pre-excavation to a depth of -3.0 m	(A-L)	
04	P	wall installation		[35]
05	P	2nd pre-excavation to a depth of -4.3 m (A-F)	[14]	
06	P	Bored concrete pile installation		[7]
07	P	tied back anchors installation	(C-E)	
08	C	1st excavation to a depth of -5.4 m	(C-E)	[0.25]
09	C	2nd excavation to a depth of -7.0 m	(C-E)	[0.25]
10	P	3rd exc. to -8.4 m and temp. strut installation	(C-E)	
11	C	consolidation time		[0.25]
12	C	4th exc. to -9.9 m and lean concrete slab inst.	(C-E)	[0.25]
13	P	anchors and temp.strut deinstallation and new strut inst.		
14	C	consolidation time		[13]
15	P	Reinforced concrete bottom slab installation		
16	C	consolidation time		[16]
17	P	1st exc. to a depth of -5.4 m and strut inst.	(E-F)	
18	C	consolidation time		[0.25]
19	C	2nd excavation to a depth of -7.0 m	(E-F)	[0.25]
20	P	3rd exc. to -8.4 m and temp. strut inst.	(E-F)	
21	C	consolidation time		[0.25]
22	C	4th exc. to -9.9 m and lean concrete slab inst.	(E-F)	[0.25]
23	P	temp. strut deinstallation		
24	C	consolidation time		[11]
25	P	Reinforced concrete bottom slab installation		
26	C	consolidation time		[14]
27	P	strut installation		
28	C	1st excavation to a depth of -5.4 m	(A-C)	[0.25]
29	C	2nd excavation to a depth of -7.0 m	(A-C)	[0.25]
30	P	3rd exc. to -8.4 m and temp. strut installation	(A-C)	
31	C	consolidation time		[0.25]
32	C	4th exc. to -9.9 m and lean concrete slab inst.	(A-C)	[0.25]
33	P	temp. strut deinstallation		
34	C	consolidation time		[20]
35	P	Reinforced bottom slab installation		
36	C	consolidation time		[8]

N.B.: P: plastic calculation; C: consolidation analysis; numbers in () are the axes containing the excavation strips according to Fig. 6; [] are consolidation and execution time

The initials stresses are generated using the gravity loading option because the non-horizontal soil layers. For all calculation phases a ground water flow calculation was performed considering the ground water level at a depth of -3 m below the ground surface on the soil side and the lower water level on the excavation side corresponding to each excavation level in the subareas of the excavation. The undrained material behaviour was ignored during the calculations phases 01 to 04. The

rest of the calculation phases are carried out using the consolidation analysis option. For the consolidation anylysis of the phases, which includes the switching on or off of the structural elements, a plastic calculation was first performed before the consolidation analysis.

In order to consider the spatial effect of the stepwise excavation in three strips, the excavation in each strip was divided in 4 excavation stages. Moreover, the spatial effect was taken in to account by introducing a partial mobilization factor of 0.5 (*Gebreselassie 2003; Kempfert/Gebreselassie 2006*), i.e., 2 m excavation in reality, for example, means a 1 m pure excavtion followed by the rest 1 m excavation and a simultaneous activation of the temporal struts or the bottom slabs in the calculation.

Calculation variations

Three variations were carried out using different soil parameters from different sources. The reference case (case 1) was calculated using the soil parameters from Table 2. All the parameters are adopted from the geotechnical report of this project, except that a modification was made on the stiffness parameters for the upper lacustrine clay layer in reference to a report from an actual project in immediate neighbourhood.

In a further variation (case 2) the material parameters for the upper lacustrine clay were modified as shown in Table 6 based on authors own experience in similar adjacent projects (*Gebreselassie 2003; Gebreselassie/Kempfert 2004; Kempfert/ Gebreselassie 2006).* Although there are contradictory opinions regarding the determination of effective shear strength parameters of soft soils in the laboratory, a cohesion part was found in all the samples tested in the laboratory. Therefore, the effective shear strength parameters were adopted here, which are determined from triaxial tests on samples taken from immediate surroundings. The secant modulus E_{50} of the soft lacustrine clay was slightly smaller, whereas the un/reloading modulus E_{ur} = 5.4 E_{50} remains almost the same as the reference case. The constrained modulus E_{oed} is smaller by about 33% compared to the reference case.

Table 6. Modified soil parameters for the HSM (Case 2)

Soil parameter for the upper lacustrine clay	
φ´	26.2°
c'	13.65 kN/m²
E_{50}^{ref}	4.472 MN/m²
E_{oed}^{ref}	3.317 MN/m²
E_{ur}^{ref}	24.076 MN/m²

Furthermore, a third variation (case 3) was included with the original stiffness parameters for the upper lacustrine clay layer from the geotechnical report, i.e., E_{50} = E_{oed} = 3.0 MN/m² and E_{ur} = 15.0 MN/m². Here the stiffness parameters are smaller by about 40 % compared to the reference values.

Analysis results and comparison with measured values

Wall deflection. In the following the computation results are presented for the main excavation phases (excavation part I), in order to show the mutual influence of the stepwise excavation of the three excavtion strips in this part on the wall deformations. The numerical results are compared with measured deformations at monitoring section MQ 3 in Axis A.

After the 2nd pre-excavation to a depth of -4.3 m (phase 05), in which the sheet pile walls remained unsupported, the outer walls (Axis A and F) are deformed towards the excavation, whereas the inner walls (axis C and E) showed insignificant deformations (Fig. 13). Because of the small excavation relief, the influence of the different material parameters on the deformation results is still insignificant at this stage. Due to the 3 m high slope (berm) behind the outer sheet pile wall in the Axis A, a wall head horizontal displacement of u_x = 7.0 cm was obtained for the reference case. The corresponding measured displacement at wall head was 4.7 cm. A displacement of 5.0 cm was added to that recorded from inclinometer, because it was observed from geodetic measurements that the soil near the inclinometer was displaced by this amount, which is not felt by the inclinometer because of the relatively rigid concrete pipe used to protect the inclinometer.

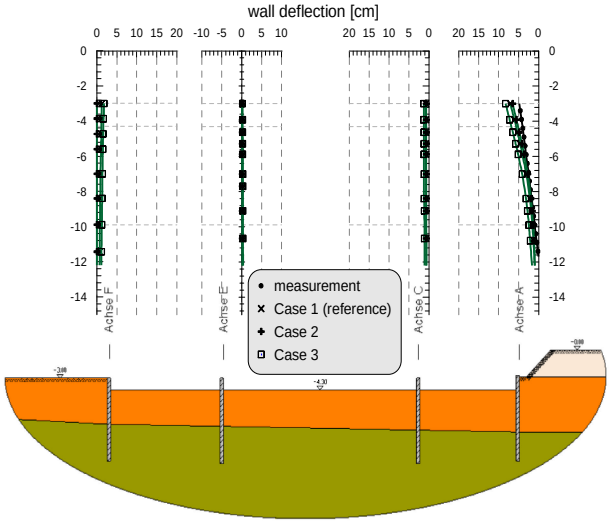

Fig. 13. Wall deflection at MQ3 after calculation phase 05

Figure 14 shows the excavation of the middle strip between Axes C and E. Before the beginning of the excavation, the

walls in these axes were tied back to the outer walls using a steel rod anchor so that a cofferdam effect would prevail. The support of the walls in this strip is dependant on the flexural rigidity and the degree of restraining of the outer walls. At the wall head, a horizontal deflection increment Δu_x = 0.8 and 0.7 cm is calculated for the reference case in the Axes F and E respectively. Similarly, Δu_x = 4.7 and 4.4 cm were obtained in the Axes A and C respectively. The horizontal deformation u_x = 5.1 cm at the wall head in the Axis C is found to be about 0.74 % the excavation depth H = 6.9 m for the reference case.

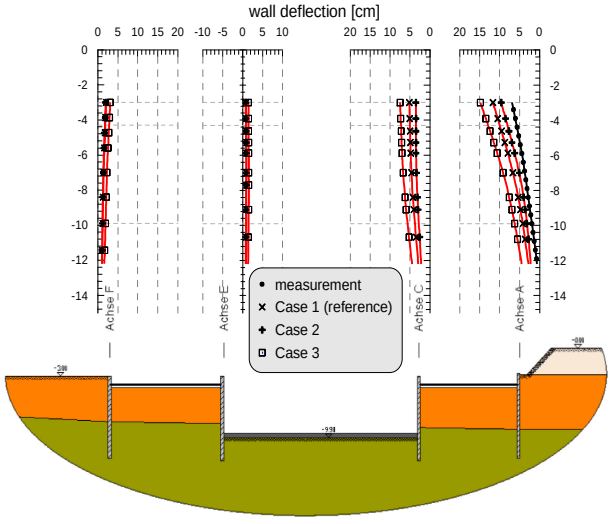

Fig. 14. Wall deflection at MQ3 after calculation phase 12

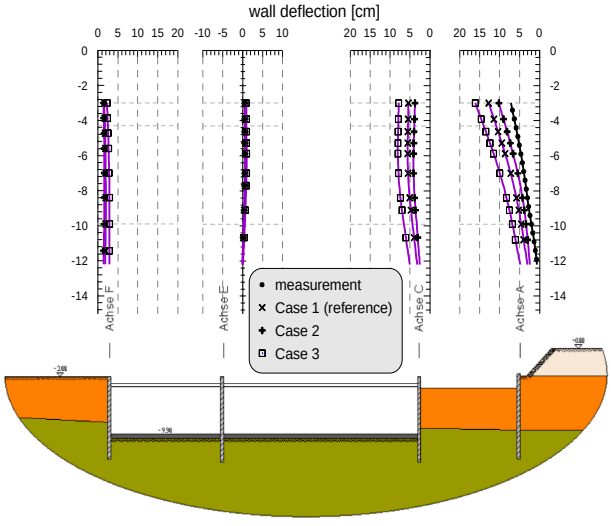

Fig. 15. Wall deflection at MQ3 after calculation phase 22

Simultaneous with the excavation of the outer strip (left on the Figure) between Axes E and F (Fig. 15) of the excavation part I, the struts were already in position, so that a force coherent connection would be possible between the wall in Axis F and the wall in Axis C through the wall in Axis E. Following the excavation in this part, both wall toes in Axes F and E were displaced towards the excavation in this strip. At the bottom of the excavation level, a horizontal deformation u_x = 0.7 cm was estimated for both walls. This leads in connection with the strut support at the wall head to a backward rotation of the wall head in the Axis F and thus a displacement of the rest of the walls towards the wall in Axis F was happened. Although no direct constructional connection was available with the sheet pile walls in the opposite outer strip (Axes A-C), about 8% increase of the wall head displacement was observed for the reference case due to the deflection of the wall in Axis C and the corresponding relief in the strip A-C.

Figure 16 shows the completion of excavation part I and the corresponding deflection of the walls. The strut supports of the sheet pile wall in the strip between the axes A and C were already installed before the start of the excavation in this strip. Horizontal deflection increment Δu_x = 5.8 and 3.2 cm was calculated at the excavation bottom for the reference case and case 2 respectively. Whereas only Δu_x = 2.8 cm was recorded from the inclinometer measurement at the same depth. On the other hand a very good agreement was achieved between calculated horizontal deformation Δu_x = 11.5 cm and measured Δu_x = 11.3 cm at wall top for case 2, which is 1.6% of the depth of excavation (H = 6.9 m).

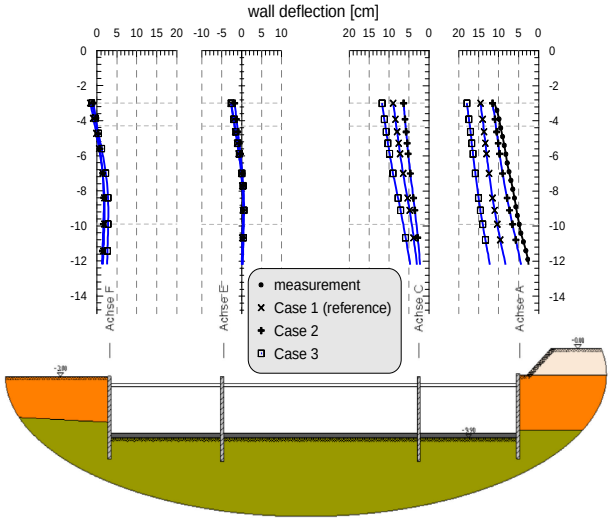

Fig. 16. Wall deflection at MQ3 after calculation phase 32

Pore Pressure. A comparative presentation of the measured and calculated pore pressure at the cross-section through the monitoring section MQ3 is indicated in Fig. 17 for the reference case only, because the other two variations did not lead to a significant change in the pore pressure development. At a depth of -13 m below the ground surface the pore pressure behind the wall dropped continuously during the excavation starting from the pre-excavation at a depth -4.3 m till the bot-

tom of excavation. About 6 weeks after the completion of the excavation part I, the pore pressure stabilizes itself to its hydrostatic condition. On the other hand a small pressure difference of about 10 kN/m² remained at a depth of -17 m because of a longer drainage path.

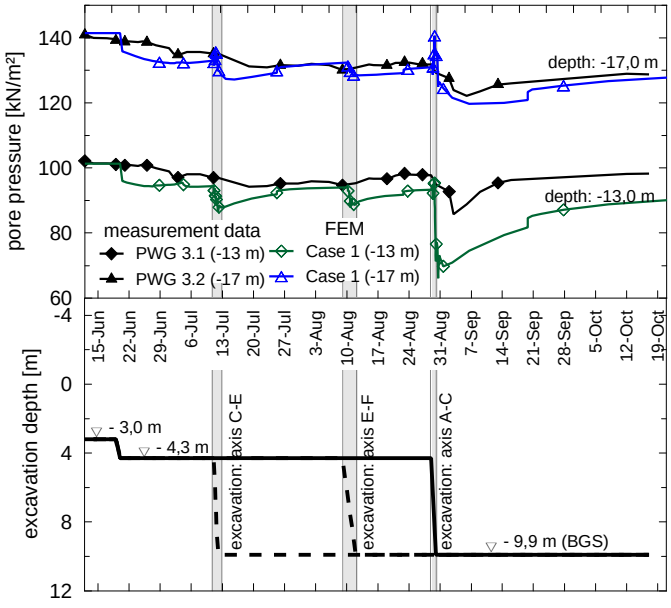

Fig. 17. Pore pressure at MQ3

Generally, it appears that the excess pore pressure due to the full excavation decomposes very slowly. The excavation of the adjacent strip between the Axes A and C lead to a reduction of the pore pressure. The numerical computation results are characterised by a substantial short period reaction time, however, a good agreement can be witnessed between the calculated and measured values from Fig. 17. The presentation of the development of the excess pore pressure in Fig. 18 shows clearly the influence of the excavation of the strip between the Axes A and C.

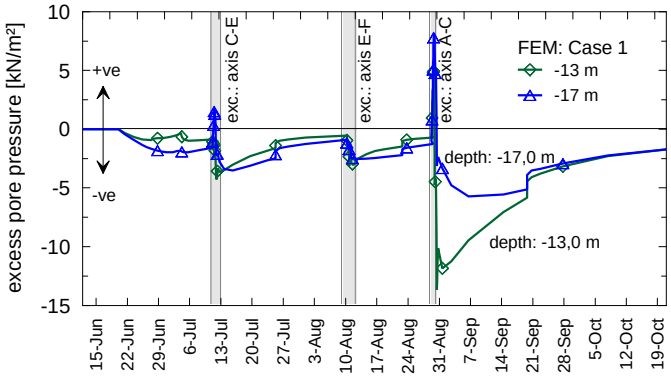

Fig. 18. Excess pore pressure at MQ3

Ground settlement and horizontal movements behind the wall. The maximum settlement u_z = 16.0 cm was occurred at MQ 2 behind the wall at the slope crust (Fig. 19), whereas only u_z = 7.0 cm settlement was recorded 4.4 m behind the wall at MQ3. As before a very good agreement was achieved between measured and calculated settlements for case 2.

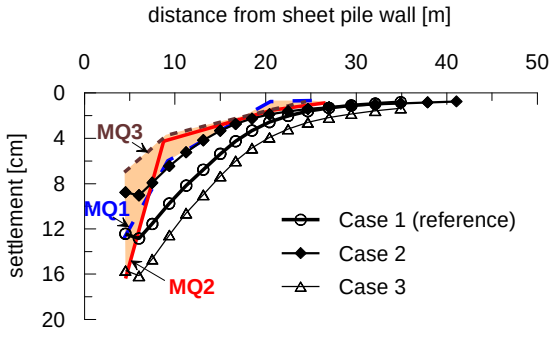

Fig. 19. Ground settlement behind the wall

Figure 20 shows the normalised settlement trough behind the wall at the ground surface according to *Peck (1969)* for different underground conditions. It appears from Fig. 20 that the calculated settlement for the case 2 corresponds approximately to the transition from zone 3 to zone 2. Similar to the wall deflection, the calculation variants using the material parameters from geotechnical report of the project (case 1 and 3) reflect the measured settlement inadequately. First after the increase of the shear strength of the soft layers (case 2) based on an intensive triaxial test result from area adjacent to the project site provides the computation a comparable settlement with that measured.

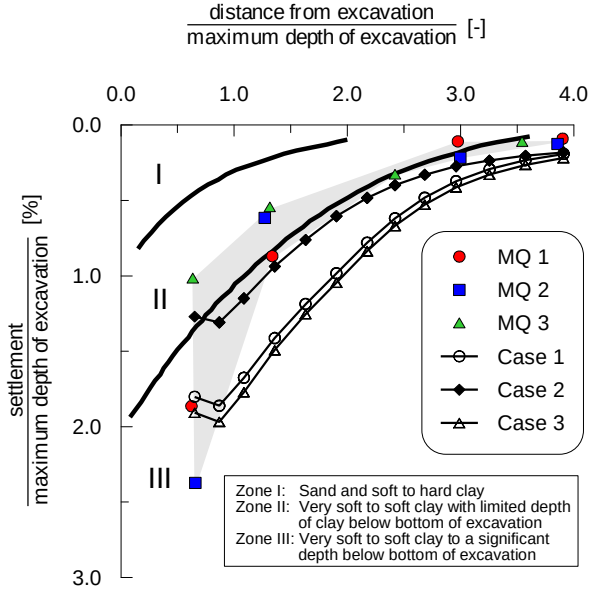

Fig. 20. The location of the settlement trough in the dimensionless diagramm by Peck (1969)

The measured horizontal deformations of the ground surface are only available up to 10 m behind the wall (Fig. 21). The maximum deformation u_x = 14.6 cm occurred at MQ2, whereas u_x = 9.2 cm was measured 4.4 m behind the wall at MQ2. As already mentioned above, the numerical computation using the material parameters according to case 2 can cover well the range of the measured horizontal deflection of the ground surface.

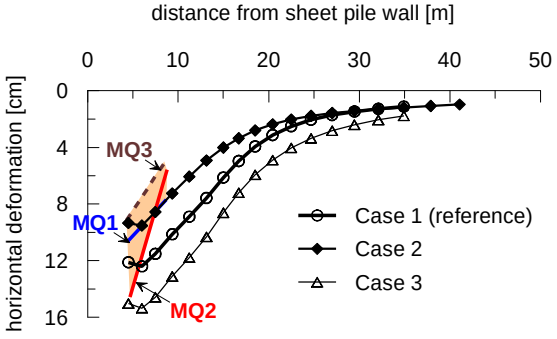

Fig. 21. Horizontal movements behind the wall

Strut forces. The reaction forces in the struts were monitored at MQ1 only. The development of the measured as well the calculated strut forces with time are indicated in Fig. 22 for the reference case. While the numerical result shows a constant strut force of 200 kN during and after the excavation of the middle strip till the beginning of excavation of the adjacent strips, the measured values varies between 250 and 100 kN. Due to these variations, no clear increase of the strut force can be observed during the excavations of the adjacent strips. It can be seen from Fig. 22 that the calculated strut forces increase by 100 and 550 kN during the excavation of the adjacent strips Axes E - F and Axes A - C respectively.

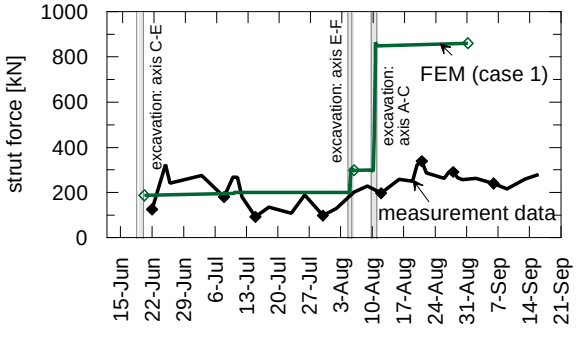

Fig. 22. strut force at MQ1

CONCLUSIONS

The simulation of the construction stages and the necessary idealization of the soil-structure-interaction has a considerable effect on the computation results. In this paper, it could be shown that by making effort to model the complex construction stages with due consideration of the real time for each excavation step and applying the consolidation analysis, a very good agreement can be attained with the measured results. Provided that the material parameters for the soft lacustrine clay would be available from reliable triaxial test results and experiences on comparable projects in the adjacent areas, the wall deformation, the pore water pressure development, the horizontal and vertical soil deformations can be predicted very well using the finite element method.

REFERENCES

BBI [2000]. *„BV Seeuferhaus Konstanz . Zusammenfassendes geotechniches Gutachten“* Hamburg, unpublished.

Bjerrum, L. [1973]. *„Problems of soil mechanics and construction on soft clay soils and structurally unstable soils (collapsible, expansive and others)”* Proceeding of the VII ICSMFE, Moscow, vol. 3, pp. 110-155.

Brinkgreve R.B.J. [2002]. *“Hand Book of the Finite Element Code for Soil and Rock Analysis, PLAXIS v8“*. A.A. Balkema, the Netherlands.

Burland, J.B. [1990]. *“On the compressibility and shear strength of natural clays”* Geotechnique 40, No. 3, pp. 329-378.

Gebreselassie, B. [2003]. *“Experimental, Analytical and Numerical Investigations of Excavations in Normally Consolidated Soft Soils“* PhD Thesis, University of Kassel, Institute of Geotechnics, No. 14.

Goldscheider, M., Gudehus, G. [1988]. *„Bau einer Tiefgarage im Konstanzer Seeton – Baugrubensicherung und Bodenmechanische Anforderungen“* Vorträge der Baugrundtagung 1988 in Hamburg, pp. 385-406.

Heil, H.M. ; Huder, J.; Amann, P. [1997]. *„Determination of shear strength of soft lacustrine clays“* Proceedings of the XIV ICSMFE, Hamburg, vol. 1, pp. 507-510.

Katzenbach, R.; Floss, R., Schwarz, W. [1992]. *„Neues Baukonzept zur verformungsarmen Herstellung tiefer Baugruben in weichem Seeton“* Vorträge der Baugrundtagung 1992 in Dresden, pp. 13-31.

Kempfert, H.-G., Gebreselassie, B. [1999]. *„Effect of anchor installation of settlement on nearby structures on soft soils“* Proc. Int. Symposium on Geotechnical Aspects of Underground Constructions in Soft Ground, Tokyo, pp. 665-670.

Gebreselassie, B., Kempfert, H.-G. [2004]. *„Excavation in Deep Soft Lacustrine Soil Deposit*" 5th International Conference on Case Histories in Geotechnical Engineering. New York.

Kempfert, H.-G.; Gebreselassie, B. [2006]. *„Excavation and Foundations in Soft Soils"* Springer-Verlag, Berlin.

Kempfert + Partner Geotechnik [2006]. *„Geotechnischer Bericht – Baugrundbeurteilung und Gründungsberatung zum Neubau Geschäftshaus Bodanstraße, Konstanz, Bericht Nr. 1+2"* Konstanz, unpublished.

Kempfert + Partner Geotechnik [2007]. *„Geotechnischer Bericht – Baugrundbeurteilung und Gründungsberatung zum Neubau Sportshaus zum See, Konstanz, Bericht Nr. 1"* Konstanz, unpublished.

Krieg, S. ; Lächler, W.; Siebler, G. [2004a]. *„Geotechnische Besonderheiten bei einer großen Baugrube mit Randbebauung in Konstanzer Seeton"* 3. Geotechniktag in München, pp. 111-129.

Krieg, S. ; Lächler, W.; Siebler, G. [2004b]. *„Tiefe Baugrube in breiigen Seetonen für das Seeuferhaus in Konstanz"* Vorträge der Baugrundtagung 2004, Leipzig, pp. 49-56.

Meißner, H. [2002]. *"Baugruben – Empfehlungen des Arbeitskreises 1.6 – Numerik in der Geotechnik, Abschnitt 3"* Geotechnik 25, pp. 44-56.

Peck, R.B. [1969]. *"Deep excavations and tunneling in soft ground. State of the Art Report"* Proc. Of the VII ICSMFE, Mexico, pp. 225-290.

Schanz, T., Vermeer, P.A., Bonnier, P.G., [1999]. "Formulation and Verification of the Hardening Soil Model" *in Beyond 2000 in Computational Geotechnics*, (R.B.J. Brinkgreve) A.A. Balkema, the Netherlands, pp. 281-290.

Scherzinger, T. [1991]. *"Materialverhalten von Seetonen – Ergebnisse von Laboruntersuchungen und ihre Bedeutung für das Bauen in weichem Baugrund"* Inst. f. Bodenmechanik und Felsmechanik der Iniversität Fridericiana in Karlsruhe, Heft 122.

Wibel + Leinenkugel [1990]. *„Altstadt - Seeufer, Bebauung Bodangelände, Konstanz - Baugrunderkundung und -beurteilung, gründungstechnische Beratung"* Kirchzarten, unpublished.

SYMBOLES AND ABBREVATIONS

γ_{sat}, γ_{unsat} = Saturated / Unsaturated unit weight

k_x, k_y = Permeability of the soil in x and y directions
c', φ' = Effective cohesion and friction angle
ψ' = Dilatancy Angle
E = Elasticity modulus
E_{50} = Secant modulus of elasticity at 50% the deviatoric failure stress
E_{oed} = Constrained modulus
E_{ur} = Modulus of elasticity for un/reloading
p^{ref} = Reference pressure (atmospheric pressure)
ν_{ur} = Poisson's ratio for un/reloading
m = Exponent in the power law of the stiffness of soil
R_f = Failure ratio
A, I = Cross sectional area and moment of inertia
w = Weight of plate per unit area
R_{inter} = Interface strength factor
ref = Reference
HSM = Hardening Soil Model
MCM = Mohr-Coulomb Model
λ_{cu} = normalized undrained shear strength
σ'_{vc} = Effektive overburden pressure
c_u = Undrained cohesion
τ_f = Vane shear strength
μ = Correction factor
H = Excavation depth
B = Excavation width
Δu_x = Increment of horizontal deformation
u_x = Horizontal deformation
u_z = Vertical deformation